Double-peak structure of the nonresonant photoresponse of terahertz quantum Hall detectors

G. Nachtwei,[1] F. Gouider,[1] C. Stellmach,[1] G. Vasile,[1,2,3] Yu. B. Vasilyev,[4] G. Hein,[5] and R. R. Gerhardts[6]
[1]*Institut für Angewandte Physik, Technische Universität Braunschweig, D-38106 Braunschweig, Germany*
[2]*Science Institute, University of Iceland, Dunhaga 3, IS-107 Reykjavík, Iceland*
[3]*National Institute of Research-Development for Cryogenics and Isotopic Technologies, RO-1000 Rm. Vâlcea, Romania*
[4]*Ioffe Physical Technical Institute, Russian Academy of Science, RUS-194021 St. Petersburg, Russia*
[5]*Physikalisch-Technische Bundesanstalt, D-38116 Braunschweig, Germany*
[6]*Max-Planck-Institut für Festkörperforschung, D-70569 Stuttgart, Germany*
(Received 18 June 2008; published 12 November 2008)

We present an approach to the double-peak structure of the nonresonant (bolometric) contribution of the photoresponse, measured as a function of the magnetic field for the optically induced breakdown of the quantum Hall (QH) effect in devices with Corbino geometry. For the optical excitation of our devices, we used a p-Ge laser continuously tunable in the wavelength range of 120 μm$\leq\lambda\leq$180 μm. In addition to the bolometric signal, we also observed peaks of the photoresponse due to the cyclotron resonance. In the theoretical part of this study, we present calculations on the basis of an electron heating model. Applying this model we provide a qualitative explanation of our experimental results. To get some insight into the amount of increase in the electron temperature of the QH system exposed to terahertz illumination, we also determined the electron temperature of the QH terahertz detector as a function of the electrical (Joule) heating. Up to about 25 μW and at a filling factor of 2, we found a linear increase in the electron temperature with the absorbed power.

DOI: 10.1103/PhysRevB.78.174305 PACS number(s): 78.67.De, 71.70.Di, 72.10.−d

I. INTRODUCTION

Terahertz (THz) radiation with wavelength on the order of $\lambda\approx120$ μm (frequency $f\approx2.4$ THz and energy $E\approx10$ meV) interacts effectively with quantum Hall (QH) systems due to the coincidence of the terahertz photon energy with the Landau gap between two adjacent Landau levels (LLs) in systems based on GaAs/AlGaAs heterojunctions.[1] The typical Landau gap developed by the QH systems investigated in this study is of the order of 10 meV. This cyclotron energy $\hbar\omega_c$ is tunable by the magnetic field B. The absorption of the terahertz radiation by the two-dimensional electron system (2DES) induces an increase in the electron temperature T_{el} relative to the lattice, detectable by the change of the conductivity. This light-induced increase in the conductivity is, in the following, called the photoresponse (PR). The electron system is very sensitive to excitations in the QH regime. Photoconductivity measurements on 2DES, excited by radiation in the terahertz range [corresponding to wavelengths in the spectral range of far-infrared (FIR) light], have been performed using the radiation of molecular gas lasers (see, for example, Ref. 2) and of a mercury lamp of a Fourier-transform-infrared (FTIR) spectrometer (see, for example, Ref. 3). There is also a variety of studies concerning measurements of the cyclotron resonance (CR) of 2DES by investigating the transmission of FIR radiation at quantum well structures (see, for example, Ref. 4).

In this study, we describe and explain the double-peak structure, as a function of the magnetic field, of the bolometric contribution to the photoresponse, which we measured on devices with Corbino geometry in quantizing magnetic fields. We observed different types of photoresponse. At the flanks of the QH plateaus, a PR double peak appears at lower values of the source-drain voltage V_{SD} [$V_{SD}\ll V_{SD}^{crit}$, V_{SD}^{crit} is the source-drain voltage at which the breakdown of the quantum Hall effect (QHE) occurs]. At higher V_{SD} values, a single peak appears, situated at that magnetic field B where also a minimum of the magnetoconductivity $\sigma_{xx}(B)$ occurs. This peak does not shift with respect to B when the energy of the incident photons is changed. In contrast, we observed at higher V_{SD} ($V_{SD}\leq V_{SD}^{crit}$) a PR peak which shifts with changing the photon energy. Whereas the signal part described first is due to bolometric heating of 2DES, the second contribution to the PR is due to the cyclotron resonance. Our explanation of the bolometric PR contribution is based on an electron heating model and on a plausible model for the dependence of the critical temperature for the breakdown of the QHE on the filling factor. This critical temperature is then compared with the elevated electron temperature resulting from energy absorption by the 2DES. In order to check our model assumptions, we also determined experimentally the electron temperature of the 2DES (i.e., the QH terahertz detector) as a function of the electrical power input. We found an approximately linear increase in the electron temperature with the electrical power input at the filling factor (FF) of $\nu=2.0$ up to temperatures of $T=4.2$ K. This indicates that the elevation of the electron temperature is due to Joule heating.

II. EXPERIMENTAL DETAILS

The samples used for this study are GaAs/AlGaAs heterostructure devices patterned in Corbino geometry. The devices have the following parameters: electron densities of $n_s=1.9\times10^{15}-2.7\times10^{15}$ m^{-2}, electron mobilities of $\mu_{el}=10-150$ m^2 V^{-1} s^{-1}, and the inner and outer radii are $r_1=500$ μm and $r_2=1500$ μm. The active medium of the terahertz laser consists of a p-doped ($p\approx10^{14}$ cm^{-3}) germa-

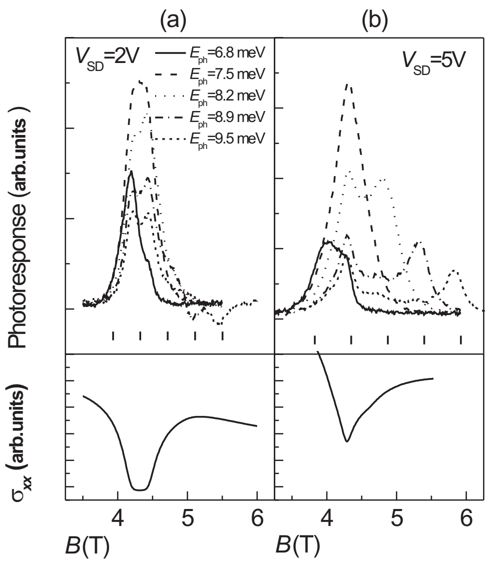

FIG. 1. Experimental traces of the measured PR vs magnetic field B for different laser energies, indicated by the vertical lines (upper panel). The transport data around filling factor of 2 vs B are shown in the lower panel. Some sample properties: $n_s = 2.0 \times 10^{15}$ m^{-2} and $\mu_{el} = 50$ m^2 V^{-1} s^{-1}. (a) $V_{SD} = 2$ V and (b) $V_{SD} = 5$ V.

nium crystal. The stimulated emission of terahertz radiation is generated by transitions inside the valence band among LLs of light holes.[5,6] The excitation terahertz source is tunable in the range of $1.7 \text{ THz} \leq f \leq 2.5$ THz corresponding to wavelengths of $180\ \mu\text{m} \geq \lambda \geq 120\ \mu\text{m}$. The laser system (terahertz source) and the QH sample (terahertz detector) are mounted on a tube, inserted in a helium (He) bath cryostat ($2.0 \text{ K} \leq T \leq 4.2$ K), and connected by a brass waveguide. The magnetic fields ($B_{laser} \leq 4$ T for the laser and $B_{sample} \leq 10$ T for the detector) are generated by superconducting coils. The electric field for the laser crystal is provided by a high power pulse generator ($1 \text{ kV} \leq V_{laser} \leq 2$ kV, $20 \text{ A} \leq I_{laser} \leq 40$ A, pulse duration time $\tau_{pulse}^{laser} \approx 1\ \mu$s).

III. BOLOMETRIC AND CYCLOTRON RESONANT CONTRIBUTIONS TO THE TERAHERTZ PHOTORESPONSE OF QUANTUM HALL DETECTORS

When a QH device is illuminated by terahertz radiation, the conductivity of the 2DES exposed to quantizing magnetic fields is affected. The illumination may cause the breakdown of the QH state into a dissipative state, which can be indicated by a photoresponse. Recent investigation of the PR on GaAs/AlGaAs heterostructures patterned in Corbino geometry[7–9] showed that both bolometric effects (BO) and cyclotron resonance contribute to the PR. The PR is measured versus the magnetic field B for different photon (laser) energies E_{ph} and exhibits a nonresonant BO contribution (single or double-peak structure) located at the minimum of the longitudinal conductivity [see Fig. 1(a)]. At higher source-drain voltages V_{SD} ($V_{SD} = 5$ V, $V_{SD} > V_{SD}^{crit}$), there occurs an additional peak, which changes its position on the B scale with E_{ph} and represents the CR contribution [see Fig. 1(b); for details, see Refs. 9 and 10]. The PR was determined from measuring the difference $\Delta\sigma_{xx} = \sigma_{xx}(\text{excited}) - \sigma_{xx}(\text{unexcited})$.

In order to understand the BO contribution to the PR, we make the plausible assumption that the energy ΔE absorbed by the 2DES during one laser pulse is proportional to the product of the power density $I_{ph} = P_{laser}/A_{photo}$ and the pulse length $\Delta\tau$ of the laser, and of the radiation-exposed area A_{photo} of the 2DES,

$$\Delta E = \alpha I_{ph} \Delta\tau A_{photo} = A_{photo} c_n \Delta T. \quad (1)$$

Here α is a proportionality constant, and we assume the transformation of the absorbed energy into heat resulting in an increase in the electron temperature by ΔT. Here, c_n is the specific heat of the 2DES at constant electron density. From Eq. (1), the temperature enhancement ΔT can be calculated:

$$\Delta T = \frac{\Delta E / A_{photo}}{c_n}. \quad (2)$$

The electron specific heat in three-dimensional (3D) metals is given by the Sommerfeld relation,

$$c_n = \frac{\pi^2}{3} k_B^2 D(E_F) T, \quad (3)$$

with $k_B = 1.3807 \times 10^{-23}$ J/K (Boltzmann's constant) and $D(E_F)$ as the density of states (DOS) at the Fermi energy. With this relation we obtain for an enhancement of the electron temperature

$$\Delta T = \frac{3\Delta E / A_{photo}}{\pi^2 k_B^2 D(E_F) T}. \quad (4)$$

The Sommerfeld relation [Eq. (3)] is valid for metals with $k_B T \ll E_F$ and nearly constant DOS on the scale of $k_B T$. We think it is reasonable to apply its analog, with $D(E_F)$ replaced by the filling-factor-dependent thermodynamic DOS $D(\nu) = dn_{el}/d\mu$, also to our 2DES although the filling-factor dependence of the specific heat of a Landau-quantized 2DES with high mobility, i.e., narrow Landau levels, at low temperature is more complicated. We have, however, indications that the effective Landau-level broadening in our Corbino devices is relatively large. In the case of a 2DES of $\mu_{el} = 50$ m^2/V s in a magnetic field of $B = 4.3$ T, (which corresponds to the Landau-level FF $\nu = 2$; see Fig. 1) at a temperature of $T = 4.2$ K, the thermal broadening $\Delta E_{th} = k_B T = 0.35$ meV is only slightly smaller than the level broadening $\Gamma = 0.41$ meV. Since $\Delta E_{th} \ll \Gamma$ is required for the applicability of the Sommerfeld expression for the specific heat, we therefore should not expect a quantitative agreement of results calculated on the basis of Eq. (3) with the measured PR. However, the electron mobility μ_{el} observed in our Corbino geometry was only one-fifth or even less of that measured at Hall bars of the same wafer.[9,10] Furthermore, both higher source-drain voltages V_{SD} ($V_{SD} \sim V_{SD}^{crit}$) and the exposure of the samples to terahertz radiation result in a less sharp structure of the DOS (increased value of Γ). Thus, the effective value of Γ in our experiments will be considerably larger than the $\Gamma = 0.41$ meV estimated above. Therefore, we

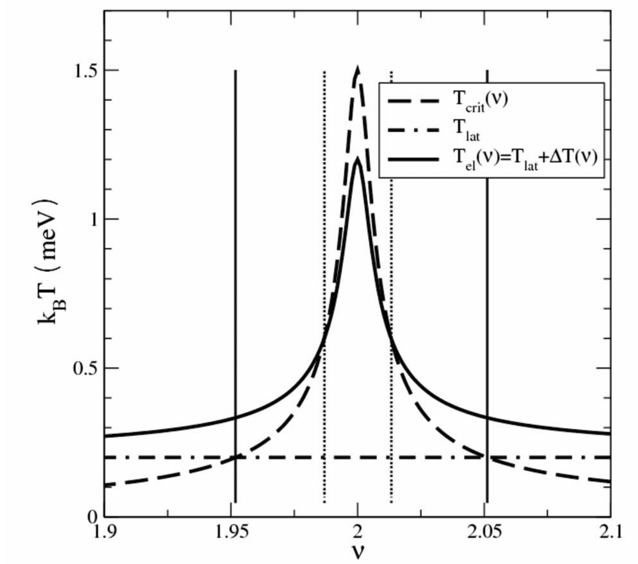

FIG. 2. Model calculation of the electron $T_{el}(\nu)$ and the critical temperatures $T_{crit}(\nu)$ near $\nu=2$, according to Eqs. (5) and (7), respectively. For $k_BT_{lat}=0.2$ meV, $K=1$ meV$\times D(\nu=2)/k_B$, and $n_s=2.42\times 10^{11}$ cm^{-2}.

can assume that the conditions for the applicability of Eq. (3) are approximately fulfilled under these conditions. Consequently, we adapt Eq. (4) to the case of our interest and assume that the absorption of radiation leads to an elevated electron temperature which can be written in the form

$$T_{el}(\nu) = T_{lat} + \Delta T(\nu), \quad \Delta T(\nu) = \frac{K}{D(\nu)}, \tag{5}$$

where T_{lat} is the background temperature of the GaAs lattice, $D(\nu)=dn_{el}/d\mu$ is the thermodynamic density of states (TDOS) at the filling factor of $\nu=2\pi l_B^2 n_{el}$ (with the magnetic length $l_B=\sqrt{\hbar/m\omega_c}$), calculated at fixed magnetic field and fixed temperature (we will take $T=T_{lat}$), and $K=3\Delta E/(A_{photo}\pi^2 k_B^2 T_{lat})$ is a constant. A numerical evaluation of Eq. (5) based on a Gaussian ansatz for the collision broadened (spin-degenerate) Landau DOS

$$D_G(E) = \frac{1}{\pi l_B^2}\sum_n \frac{1}{\Gamma\sqrt{\pi}}\exp(-[E-\hbar\omega_c(n+1/2)]^2/\Gamma^2), \tag{6}$$

with a magnetic-field-dependent level broadening $\Gamma = \sqrt{2/\nu}1.8$ meV is depicted in Fig. 2 (solid line). The calculated temperature increase is largest at the filling factor $\nu=2$, where the TDOS $D(\nu)$ has a minimum.

This does not, however, yet explain the double-peak structure of the PR with two maxima near the flanks of the QH plateau [see Fig. 1(a)]. To understand this, we compare the elevated electron temperature $T_{el}(\nu)$ with the critical temperature $T_{crit}(\nu)$ at which the QHE breaks down. To get an estimate for T_{crit} as a function of the filling factor, which describes the decrease in T_{crit} with increasing distance of ν from the integer value $\nu=i$, we use the ansatz

$$T_{crit}(\nu) = \frac{T_{crit}(i)D(i)}{D(\nu)}, \tag{7}$$

where $T_{crit}(i)$ is the critical temperature and $D(i)$ is the TDOS at the integer filling factor $\nu=i$. Assuming further the validity of the hot-electron model $\sigma(T_{el})=\sigma(T_{lat}+\Delta T)$, the magnitude of $\Delta\sigma_{photo}=\sigma(T_{lat}+\Delta T)-\sigma(T_{lat})$ can be understood from a comparison (i.e., without radiation): the 2DES is at the temperature $T=T_{lat}$. If $T<T_{crit}(\nu)$, i.e., between the vertical solid lines in Fig. 2, the 2DES is in the QH state. Outside of this interval, i.e., for $\nu\leq 1.95$ and $\nu\geq 2.05$, the 2DES is in the high-resistive normal state since $T>T_{crit}(\nu)$. After illumination the 2DES is at the temperature $T_{el}(\nu)$, given by the solid line in Fig. 2, which intersects the $T_{crit}(\nu)$ curve at the two values indicated by the dotted vertical lines. In between these dotted lines, the resulting elevated temperature $T_{el}(\nu)<T_{crit}(\nu)$ is still lower than the critical temperature. As a consequence, in this interval centered around $\nu=i=2$, the 2DES after illumination remains in the QH state and the PR is negligibly small. In the ν intervals between the solid and the dotted vertical lines, the illumination increases the temperature from $T=T_{lat}<T_{crit}(\nu)$ to $T_{el}(\nu)>T_{crit}(\nu)$, and the 2DES is driven by the radiation heating out of the QH state into the normal state, which is accompanied by a considerable PR. For ν values outside the interval marked by the solid vertical lines, the 2DES is heated a little within the normal state and the PR is again relatively small. Thus, the comparison of $T_{el}(\nu)$ and $T_{crit}(\nu)$ shows that the PR has two maxima at both sides of the integer filling factor (here $\nu=i=2$), i.e., at the flanks of the QH plateau, where the heating by the laser radiation leads to a breakdown of the QHE. In the numerical calculation (see Fig. 2), the values of the level broadening and of the critical temperature $T_{crit}(\nu=2)$ may have been overestimated. Also, for consistency reasons, $D(\nu)$ should have been calculated self-consistently at the elevated temperature $T_{el}(\nu)$ and not at T_{lat}. We, however, believe that such quantitative corrections will not change our picture qualitatively and that Fig. 2 explains the relevant physics of the observed double-peak structure correctly.

To explain the further reduction in $\Delta\sigma_{photo}$ toward the Shubnikov–de Haas (SdH) maxima is beyond this simple qualitative model. However, it becomes evident if we again employ the hot-electron model since, first, the temperature increase ΔT becomes smaller as $D(\nu)$ increases toward its maxima at half-filled Landau levels. Second, within the conventional transport theories, i.e., the self-consistent Born approximation (SCBA) (Refs. 11 and 12) or a similar theory related to the Gaussian DOS of Eq. (6),[13,14] which are based on the interaction of the 2DES with randomly distributed impurities (ionized donors), the SdH maxima of the longitudinal conductivity decrease with increasing temperature.[12,14] With this in addition to the comparison described above, the double-peak structure of $\Delta\sigma_{photo}(\nu)$ observed in our experiments is well explained by the picture based on Eqs. (5) and (7).

In addition to the nonresonant contribution to the PR described above, at higher V_{SD} values we observe also a contribution due to the CR [for $V_{SD}=5$ V$>V_{SD}^{crit}(\nu=i=2)$; see

Fig. 1(b)]. In contrast to the BO peak (which is situated independently of the energy of the incident photons near the B value corresponding to integer filling factor, here $\nu=2$), the CR peak shifts on the B scale when the energy of the photons E_{ph} emitted by the p-Ge laser is changed. A plot of this B position (B_{CR}) as a function of E_{ph} yields a cyclotron mass m_{CR} equal to the effective mass m^* of electrons in GaAs according to

$$E_{ph} = \hbar\omega_{ph} = \hbar\frac{eB_{CR}}{m_{CR}}. \tag{8}$$

The CR peaks are observable clearly only at noninteger filling factors $\nu \neq 2$ and at higher values of the source-drain voltage ($V_{SD}=5$ V). This is because delocalized carriers are necessary to observe the CR.

For a direct experimental justification of the model calculation presented in Fig. 2, a measurement of the filling-factor dependence of the critical temperature $T_{crit}(\nu)$ and of the elevated electron temperature $T_{el}(\nu)$ would be desirable. Of course, there is experimental indication that $T_{crit}(\nu)$ has a maximum at integer filling factor but a direct measurement near the center of the QH plateau is not possible with our setup. The concept of an elevated electron temperature $T_{el}(\nu)$ resulting from the absorption of laser energy is based on the model assumption that, under the illumination, a power balance between absorbed laser energy and loss energy transferred to the lattice is established, leading to a stationary state which can be described by this elevated temperature $T_{el}(\nu)$ (for a detailed discussions, see Refs. 15–17). If this electron heating model is correct, the transport coefficients in this stationary state should depend only on this electron temperature and not on the manner in which this temperature was established. To check these ideas, we performed conductivity measurements at low lattice temperature T_{lat} and with increasing source-drain voltages V_{SD}, which led to a Joule heating of the 2DES, and compared the results with low-V_{SD} measurements at increasing lattice temperatures. The electron heating model assumes that the same value of the conductivity is obtained in both kinds of measurements if the electron temperatures are the same, either reached by Joule heating of the 2DES at low T_{lat} or by high T_{lat} at low current.

By using this model we can deduce the electron temperatures near the breakdown of the QHE at the filling factor $\nu=2$. To find the electron temperature, we first plot the longitudinal conductivity σ_{xx} versus the applied source-drain voltage V_{SD} and versus the temperature T, respectively. For each value of the source-drain voltage V_{SD}, we determine the temperature, which leads to the same value of the conductivity [see Fig. 3(a)]. Thus, a correspondence between the electron temperature T_{el} and the applied source-drain voltage V_{SD} is determined [see Fig. 3(b)]. The estimated electron temperature is limited to $T=4.1$ K due to the design of our experimental setup. As seen from Fig. 3(c), the electron temperature of $T_{el}=4.1$ K is reached at an input of the electrical power of $P_{electric}=25$ μW for $\nu=2$. Up to this amount, T_{el} increases approximately linearly with $P_{electric}$. This indicates that Joule heating is responsible for the value of T_{el}. To check this linearity of the function $T_{el}(P_{electric})$ at $P_{electric}>25$ μW, sample temperatures of $T>4.1$ K are needed. Unfortunately, with our experimental setup, it is impossible to stabilize temperatures of $T>4.1$ K inside the laser chamber, where the sample is also situated. However, it would be desirable to determine $T_{el}(P_{electric},\nu)$ also for $P_{electric}>25$ μW and for $\nu\neq 2$.

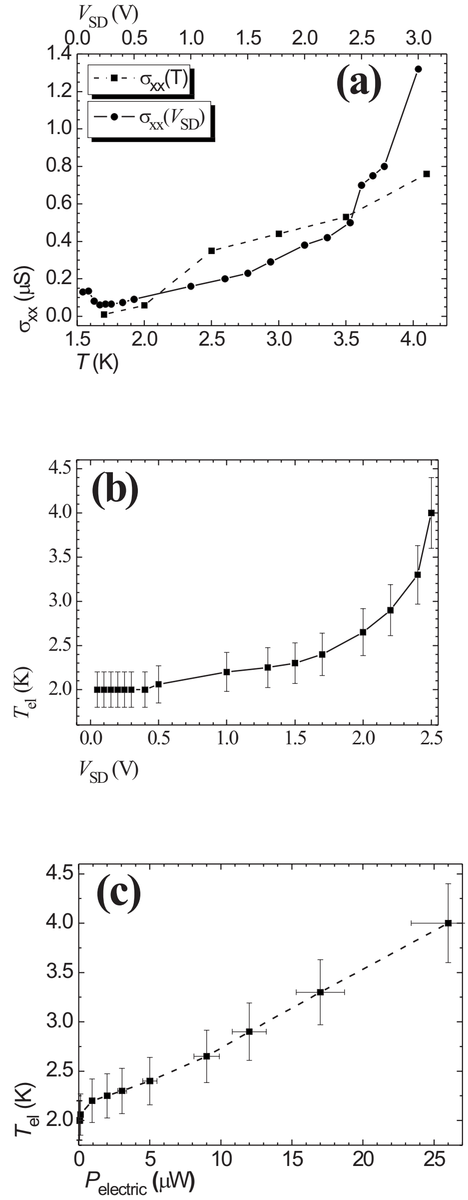

FIG. 3. (a) Temperature (dashed line) and source-drain voltage (solid line) dependences of the longitudinal conductivity σ_{xx}. (b) The electron temperature T_{el} versus the applied source-drain voltage V_{SD} near the breakdown of the QHE at $B(\nu=2.1)=4.16$ T, $T_{lat}=1.7$ K. (c) The electron temperature as a function of the electrical power determined for one of the investigated samples, $T_{lat}=1.7$ K. Some sample characteristics: $r_1=500$ μm and $r_2=1500$ μm, which are the inner and outer radii of the QH device with Corbino shape, $n_s=2.1\times 10^{15}$ m^{-2} and $\mu_{el}=50$ m^2 V^{-1} s^{-1}.

IV. CONCLUSIONS

In this study, we presented an approach based on the electron temperature picture which can qualitatively explain our

PR measurements on QH terahertz detectors. The double-peak structure of the PR measured as a function of the magnetic field can be attributed to a nonresonant bolometric response of the QH system due to the heating of the electrons by the terahertz radiation. At higher source-drain voltages, an additional peak of PR due to the cyclotron resonance is observed.

Further, as a check of the electron temperature picture used to explain the increase in the electron temperature by the optical excitation of the QH system, Joule heating experiments with increasing source-drain voltages at low lattice temperatures were performed near filling factor of 2. We observed a nearly linear increase in the electron temperature with the absorbed electric power, which supports the basic idea of our approach.

ACKNOWLEDGMENTS

We acknowledge the support of G. Vasile by the Deutsche Forschungsgemeinschaft (DFG) and by the Deutscher Akademischer Auslandsdienst (DAAD).

[1] K. von Klitzing, Rev. Mod. Phys. **58**, 519 (1986).

[2] D. Stein, G. Ebert, K. von Klitzing, and G. Weimann, Surf. Sci. **142**, 406 (1984).

[3] C. Notthoff, A. Lorke, and D. Reuter, Physica E (Amsterdam) **40**, 1328 (2008).

[4] D. Heitmann, M. Ziesmann, and L. L. Chang, Phys. Rev. B **34**, 7463 (1986).

[5] Yu. L. Ivanov and Yu. B. Vasilyev, Sov. Tech. Phys. Lett. **9**, 264 (1983).

[6] E. Gornik and A. A. Andronov, Opt. Quantum Electron. **23**, v (1991).

[7] S. D. Suchalkin, Yu. B. Vasilyev, S. V. Ivanov, and P. S. Kop'ev, Semiconductors **33**, 889 (1999).

[8] C. Stellmach, A. Hirsch, G. Nachtwei, Yu. B. Vasilyev, N. G. Kalugin, and G. Hein, Appl. Phys. Lett. **87**, 133504 (2005).

[9] C. Stellmach, G. Vasile, A. Hirsch, R. Bonk, Yu. B. Vasilyev, G. Hein, C. R. Becker, and G. Nachtwei, Phys. Rev. B **76**, 035341 (2007).

[10] C. Stellmach, Ph.D. thesis, Technical University Braunschweig, 2006.

[11] T. Ando, A. B. Fowler, and F. Stern, Rev. Mod. Phys. **54**, 437 (1982).

[12] A. Siddiki and R. R. Gerhardts, Phys. Rev. B **70**, 195335 (2004).

[13] R. R. Gerhardts, Z. Phys. B **21**, 285 (1975).

[14] K. Güven and R. R. Gerhardts, Phys. Rev. B **67**, 115327 (2003).

[15] G. Ebert, K. von Klitzing, K. Ploog, and G. Weimann, J. Phys. C **16**, 5441 (1983).

[16] S. Komiyama, T. Takamasu, S. Hiyamizu, and S. Sasa, Solid State Commun. **54**, 479 (1985).

[17] Y. Kawano, Y. Hisanaga, H. Takenouchi, and S. Komiyama, J. Appl. Phys. **89**, 4037 (2001).